Asociación Argentina
de Mecánica Computacional

Mecánica Computacional Vol XXIX, págs. 8699-8715 (artículo completo)
Eduardo Dvorkin, Marcela Goldschmit, Mario Storti (Eds.)
Buenos Aires, Argentina, 15-18 Noviembre 2010

MODELING AND SIMULATION OF GAS, OIL AND WATER FLOW IN A CATENARY-SHAPED RISER

Rafael H. Nemoto and Jorge L. Baliño

Núcleo de Dinâmica e Fluidos, Departamento de Engenharia Mecânica, Escola Politécnica da Universidade de São Paulo, Av. Prof. Mello Moraes, 2231, CEP 05508-900 - Cidade Universitária, São Paulo, SP, Brazil, rafael.nemoto@usp.br, jlbalino@usp.br

Keywords: Multiphase flow, petroleum production systems, characteristic values, no-pressure-wave model, black oil model.

Abstract. In this paper, a one-dimensional multiphase flow model in a catenary-shaped riser is presented, as well as results obtained through dynamic simulations. The model considers continuity equation for gas, oil and water phases and a simplified momentum equation without inertia terms (no-pressure-wave or NPW approximation) for the phases flowing together. Oil and water phases are considered to have the same velocity and are homogenized. Slip between the liquid and gas phases are taken into account by using a drift flux model. Mass transfer between the oil and gas phases are calculated using the black oil model. The numerical solution of the equations is obtained using the method of characteristics. As result of the simulations, the evolution of the pressure at the bottom of the riser is shown for different inflow boundary conditions.

1 INTRODUCTION

There are many works in literature that present different models for air-water flow in pipeline-riser systems. Schmidt et al. (1979), Fabre et al. (1987), Taitel et al. (1990), Sarica and Shoham (1991) and Baliño et al. (2010) are some of the authors that researched the behavior of this biphasic flow and proposed different methods to determine the system stability. A stable system is one in which slug and bubble flow are observed in the riser and a unstable flow is related to the occurrence of the severe slugging phenomenon.

Using air-water as flowing fluids in pipeline-riser systems, it is possible to investigate basic mechanisms that influence the stability; however, there are many limitations when trying to extrapolate these results to petroleum production systems:

- Pipeline lengths and riser heights in petroleum production systems are much bigger (order of kilometers long) than the values for air-water experimental facilities. The high pressure ratios between the bottom and top of the riser give rise to important expansion effects in the gas phase, invalidating models based on the assumption of a mean void fraction.

- Petroleum is a multicomponent system in which both liquid and gas phases coexist at operating conditions (McCain, 1990). Mass transfer between the phases are dependent on pressure and temperature through the PVT curve. With the high pressure variations in the riser, mass transfer effects cannot be ignored. Besides, the fluid coming from the reservoir has a water content, so three phases can coexist in the general case.

- Most of the experiments in air-water systems were realized keeping a constant separation pressure as a boundary condition. A few experiments investigated the effect of a choking valve at the top of the riser. Because of the low pressures involved, the valve operated in subcritical conditions. In petroleum production systems, a choke valve located at the top of the riser normally operates in critical conditions.

In this paper a one-dimensional model for gas, oil and water flow in a catenary-shaped riser is presented. This model is based on the previous work of Baliño et al. (2010), incorporating aspects that are important in petroleum production systems, as the evolution of the gas as a real gas, mass transfer between the oil and gas phases and a choke valve at the top of the riser that can operate in the critical or subcritical state.

The pipeline model is under development and it will be linked to the riser model. Then it will be possible to study the entire system working together and evaluate stability maps to operational conditions related to real offshore production systems.

2 MULTIPHASE FLOW MODEL

The model is based on one-dimensional three-phase isothermal flow. It considers continuity equation for gas, oil and water phases and a simplified momentum equation without inertia terms for the phases flowing together. Oil and water phases are considered to have the same velocity and are homogenized. Slip between the liquid and gas phases are taken into account by using a drift flux model. Mass transfer between the oil and gas phases are calculated using the black oil model. The liquid and gas phases are assumed to be compressible and the gas behaves as a real gas. Solubility of gas and vaporization are neglected for water.

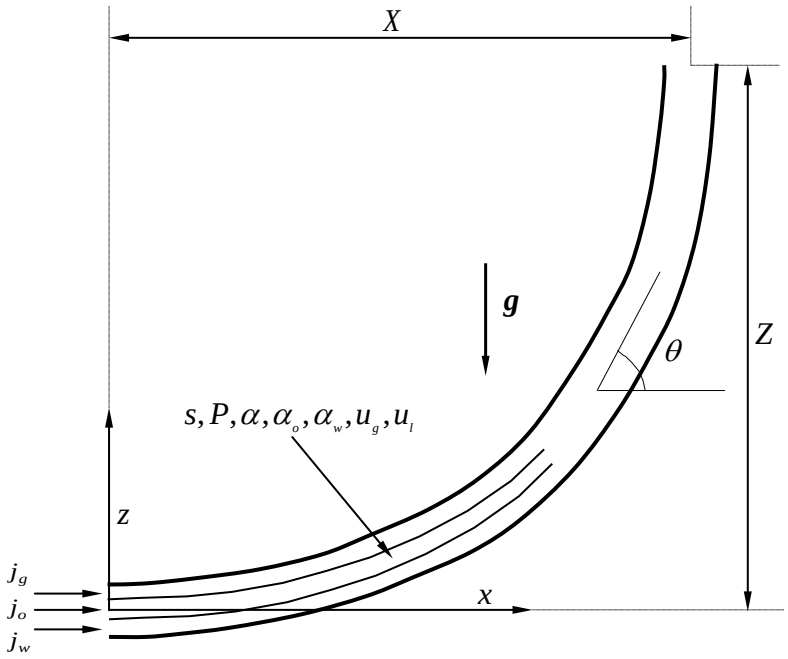

Figure 1: Definition of variables at the riser.

2.1 Riser geometry

The catenary geometry is characterized by the coordinates X and Z, corresponding to the abscissa and the height of the top of the riser (see Fig. 1). It is assumed that the inclination angle at the bottom is zero.

The local height z of a point belonging to catenary can be written as:

$$z = \varphi \left[\cosh\left(\frac{x}{\varphi}\right) - 1 \right] \tag{1}$$

where the dimensional catenary constant φ is obtained as the solution of the following transcendental equation:

$$Z = \varphi \left[\cosh\left(\frac{X}{\varphi}\right) - 1 \right] \tag{2}$$

The local position s along the catenary results:

$$s = \varphi \sinh\left(\frac{x}{\varphi}\right) \tag{3}$$

The local inclination angle θ can be written as:

$$\theta = \arctan\left[\sinh\left(\frac{x}{\varphi}\right)\right] \tag{4}$$

Knowing the position s, the local abscissa x can be calculated from Eq. (3):

$$x = \varphi \operatorname{arcsinh}\left(\frac{s}{\varphi}\right) \tag{5}$$

2.2 Conservation equations

Considering continuity equations for the phases oil, gas and water, we get:

$$\frac{\partial}{\partial t}(\rho_g\,\alpha) + \frac{\partial j_g}{\partial s} = \Gamma \tag{6}$$

$$\frac{\partial}{\partial t}(\rho_o\,\alpha_o) + \frac{\partial j_o}{\partial s} = -\Gamma \tag{7}$$

$$\frac{\partial}{\partial t}(\rho_w\,\alpha_w) + \frac{\partial j_w}{\partial s} = 0 \tag{8}$$

where s is the coordinate along the flow direction, t is time, ρ_g, ρ_o and ρ_w are the densities of the phases (correspondingly gas, oil and water), j_g, j_o and j_w are the superficial velocities, α, α_o and α_w are the volume fractions and Γ is the vaporization source term.

In most of the transients occurred in oil and gas transport, for instance in severe slugging, the response of the system proves to be relatively slow, showing that pressure waves do not have a strong effect on the initiation and transport of void waves. In the no-pressure-wave (NPW) model (Masella et al., 1998), acoustic waves are ruled out by neglecting inertia terms from the momentum equation, resulting an algebraic relation for the pressure gradient:

$$\frac{\partial P}{\partial s} = -\frac{4\,\tau_w}{D} + \rho_m\,g_s \tag{9}$$

$$\rho_m = \rho_g\,\alpha + \rho_o\,\alpha_o + \rho_w\,\alpha_w \tag{10}$$

where P is pressure, ρ_m is the density of the mixture, D is the pipe diameter, g_s is the gravity component in the s-direction and τ_w is the mean shear stress at the pipe wall. The volume fractions are related by:

$$\alpha_o + \alpha_w + \alpha = 1 \tag{11}$$

2.3 Closure laws

In order to close mathematically the problem, some simplifications must be made.

2.3.1 Homogenization of liquid phases

Assuming equal velocities for oil and water, we obtain:

$$j_o = j_l\,\frac{\alpha_o}{1-\alpha} \tag{12}$$

$$j_w = j_l\,\frac{\alpha_w}{1-\alpha} \tag{13}$$

$$j_l = j_o + j_w = u_l\,(1-\alpha) \tag{14}$$

where j_l and u_l are correspondingly the superficial velocity and the velocity of the liquid (oil plus water) phase.

2.3.2 Shear stress at the wall

The shear stress at the wall is estimated using a homogeneous two-phase model and the correlation from Chen (1979) for the Fanning friction factor f, resulting the following relations:

$$\tau_w = \frac{1}{2} f_m \rho_m j \ |j| \tag{15}$$

$$f_m = f\left(Re_m, \frac{\epsilon}{D}\right) \tag{16}$$

$$f\left(Re, \frac{\epsilon}{D}\right) = \left\langle -4\log_{10}\left\{\frac{1}{3,7065}\frac{\epsilon}{D} - \frac{5,0452}{Re}\log_{10}\left[\frac{1}{2,8257}\left(\frac{\epsilon}{D}\right)^{1,1098} + \frac{5,8506}{Re^{0,8981}}\right]\right\}\right\rangle^{-2} \tag{17}$$

$$Re_m = \frac{\rho_m D \ |j|}{\mu_m} \tag{18}$$

$$\mu_m = \mu_o \alpha_o + \mu_w \alpha_w + \mu_g \alpha \tag{19}$$

$$j = j_o + j_w + j_g \tag{20}$$

where Re_m and μ_m are correspondingly the Reynolds number and dynamic viscosity of the mixture, μ_o, μ_w and μ_g are the viscosities of the phases, ϵ is the pipe roughness and j is the total superficial velocity.

2.3.3 Real gas

Because of the high pressures involved, the constitutive relation for the gas phase is considered as:

$$\rho_g = \frac{\gamma_g M_a}{\Lambda T}\frac{P}{Z} \tag{21}$$

where $\gamma_g = \dfrac{M_g}{M_a}$ is the gas specific gravity, M_g and $M_a = 28.966$ are respectively the molar masses of gas and air, Z is the gas compressibility factor (dependent on pressure, temperature and gas composition) and $\Lambda = 8.314\, m^2 s^{-2} K^{-1}$ is the gas universal constant.

2.3.4 Drift flux model

The superficial velocities for the liquid and gas phases are determined by using a drift flux model (Zuber and Findlay, 1965):

$$j_g = \alpha\left(C_d\, j + U_d\right) \tag{22}$$

$$j_l = \left(1 - \alpha\, C_d\right) j - \alpha\, U_d \tag{23}$$

$$j = j_l + j_g \tag{24}$$

where the parameters C_d and U_d depend on the local geometric and flow conditions (Bendiksen, 1984; Chexal et al., 1992). In a general form, it will be assumed that $C_d = C_d\,(\alpha,\ P,\ j,\ \theta)$ and $U_d = U_d\,(\alpha,\ P,\ j,\ \theta)$, where θ is the local inclination angle of the pipe.

2.3.5 Black oil model

The vaporization term can be calculated by using the black oil model (McCain, 1990). According to this model, the gas specific gravity does not change with variations of pressure and temperature:

$$\gamma_g \cong \gamma_{g\,0} \tag{25}$$

$$\gamma_{dg} \cong \gamma_{g\,0} \tag{26}$$

where γ_g is the gas specific gravity at local conditions, $\gamma_{g\,0}$ is the gas specific gravity at standard conditions and γ_{dg} is the dissolved gas specific gravity.

In this way, many properties corresponding to the phases at operating conditions can be estimated based on parameters at standard condition (1 atm and 60 ^oF for API, American Petroleum Institute) and a set of correlations depending on pressure, temperature and composition, which will be considered as locally and instantaneously valid.

The vaporization term can be expressed as:

$$\Gamma = -\frac{\rho_{g\,0}\,\alpha_o}{B_o}\left(\frac{\partial R_s}{\partial t} + \frac{j_o}{\alpha_o}\frac{\partial R_s}{\partial s}\right) \tag{27}$$

where $\rho_{g\,0}$ is the gas density at standard condition, B_o is the oil formation volume factor and R_s is the solution gas-oil ratio. It is worth noting that for $\Gamma > 0$ must be $\alpha_o > 0$, while for $\Gamma < 0$ must be $\alpha > 0$.

2.4 Choke valve

The choke valve model is based on the work of Perkins (1993), which is valid for both critical and subcritical regime. Rastoin et al. (1997) has compared the Perkin's model to three other well-known choke valve models in literature and the Perkin's model has shown to be superior to the others for flow rate and upstream pressure predictions.

3 WELL-POSEDNESS AND METHOD OF CHARACTERISTICS

For a model to describe physical phenomena correctly it must be well-posed, this is, the solution must exist, must be uniquely determined and must depend in a continuous fashion on the initial and boundary conditions (Drew and Passman, 1999). This property is particularly important in multiphase flows, where partial differential equations of hyperbolic nature can be found; in this case, well-posedness implies that the characteristic values (eigenvalues or characteristic wave velocities) must be real.

The characteristic values of the presented system of conservation equations are given by:

$$e_1 = \frac{\partial j_g}{\partial \alpha} \quad e_2 = \frac{j_o}{\alpha_o} = u_l \quad e_3 = \infty \quad e_4 = \infty \tag{28}$$

where u_l is the liquid velocity. If the parameters C_d and U_d are not dependent of α, i.e. $C_d = C_d(P, j, \theta)$ and $U_d = U_d(P, j, \theta)$ (as in the correlation developed by Bendiksen (1984)) we have:

$$\frac{\partial j_g}{\partial \alpha} = \frac{j_g}{\alpha} = u_g \tag{29}$$

where u_g is the gas velocity.

There exists an algebraically-double eigenvalue equal to ∞, these eigenvalues are related to the pressure wave velocities. The pressure wave is propagated in negative and positive directions with an infinite velocity, meaning that any pressure change is felt by the entire system instantaneously.

The method of characteristics will be applied to solve the system of equations. This method is the natural numerical procedure for hyperbolic systems. By an appropriate choice of coordinates, the original system of hyperbolic partial differential equations can be replaced by a system of ordinary differential equations expressed in the characteristic coordinates. Characteristic coordinates are the natural coordinates of the system in the sense that, in terms of these coordinates, differentiation is simpler (Ames, 1992).

The resulting system of equations in the characteristic coordinates, or compatibility conditions, is given by:

$$b^*_{11}\,\frac{D_g\alpha}{Dt} + b^*_{13}\,\frac{D_gP}{Dt} + d^*_1 = 0 \tag{30}$$

$$b^*_{21}\,\frac{D_l\alpha}{Dt} + b^*_{22}\,\frac{D_l\alpha_o}{Dt} + b^*_{23}\,\frac{D_lP}{Dt} = 0 \tag{31}$$

where the coefficients b^*_{11}, b^*_{13}, b^*_{21}, b^*_{22}, b^*_{23} and d^*_1 are function of the state variables and dependent variables:

$$b^*_{11} = -\rho_o$$

$$b^*_{13} = \frac{\rho_o\left(\frac{\partial j_g}{\partial j} - 1\right)}{\rho_g}\left(\alpha\,\frac{\partial \rho_g}{\partial P} + \frac{\rho_{dg\,0}\,\alpha_o}{B_o}\,\frac{\partial R_s}{\partial P}\right) + \alpha_o\,\frac{\partial \rho_o}{\partial P}\,\frac{\partial j_g}{\partial j} - \frac{\rho_{dg\,0}\,\alpha_o}{B_o}\,\frac{\partial R_s}{\partial P}\,\frac{\partial j_g}{\partial j} + \frac{\rho_o\,\alpha_w}{\rho_w}\,\frac{\partial \rho_w}{\partial P}\,\frac{\partial j_g}{\partial j}$$

$$b^*_{21} = \alpha_o\,\rho_o$$

$$b^*_{22} = \rho_o\,(\alpha_o + \alpha_w)$$

$$b^*_{23} = \alpha_o\,\alpha_w\,\frac{\partial \rho_o}{\partial P} - \alpha_w\,\frac{\rho_{dg\,0}\,\alpha_o}{B_o}\,\frac{\partial R_s}{\partial P} - \frac{\alpha_w\,\alpha_o\,\rho_o}{\rho_w}\,\frac{\partial \rho_w}{\partial P}$$

$$d^*_1 = \left[\rho_o\left(\frac{\partial j_g}{\partial j} - 1\right) - \frac{\alpha_o\,\rho_o}{\alpha_o + \alpha_w}\,\frac{\partial j_g}{\partial j} - \frac{\alpha_w\,\rho_o}{\alpha_o + \alpha_w}\,\frac{\partial j_g}{\partial j}\right]\alpha\left(j\,\frac{\partial C_d}{\partial s} + \frac{\partial U_d}{\partial s}\right) +$$
$$+ (u_l - u_g)\left\{\frac{\rho_{dg\,0}\,\alpha_o}{B_o}\,\frac{\partial R_s}{\partial P}\left[\frac{\rho_o}{\rho_g}\left(1 - \frac{\partial j_g}{\partial j}\right) + \frac{\partial j_g}{\partial j}\right] - \alpha_o\,\frac{\partial \rho_o}{\partial P}\,\frac{\partial j_g}{\partial j} - \frac{\rho_o\,\alpha_w}{\rho_w}\,\frac{\partial \rho_w}{\partial P}\,\frac{\partial j_g}{\partial j}\right\}$$
$$\times\left(\tau_w\,\frac{\mathcal{P}_m}{A} - \rho_m\,g_s\right) \tag{32}$$

The directional derivatives are defined as:

$$\frac{D_g}{Dt} = \frac{\partial}{\partial t} + u_g\,\frac{\partial}{\partial s} \tag{33}$$

$$\frac{D_l}{Dt} = \frac{\partial}{\partial t} + u_l\,\frac{\partial}{\partial s} \tag{34}$$

4 FLUID PROPERTIES

The properties of fluids are calculated by analytical correlations based on experimental results and field data.

4.1 Gas formation volume factor and gas density

The gas formation volume factor is calculated by the following expression:

$$B_g = \frac{P_0}{T_0}\frac{Z\,T}{P} \tag{35}$$

where P_0 is the pressure at standard conditions, T_0 is the absolute temperature at standard conditions, Z is the compressibility factor and P and T are the pressure and the absolute temperature at local conditions.

The compressibility factor is determined using the correlation of Dranchuk and Abu-Kassem (1975), which correlates the results of the chart of Standing and Katz (1942). For the evaluation of the compressibility factor is also necessary to calculate the pseudocritical temperature and pressure, which can be determined using the correlation of Standing (1981), that was based on the charts of Brown et al. (1948).

Considering the black oil approximation, which assumes a approximately constant gas specific gravity, it can be shown that Eq. (21) reduces to:

$$\rho_g \cong \frac{\rho_{g\,0}}{B_g} \tag{36}$$

4.2 Water formation volume factor and water density

The correlation for water formation volume factor is presented in the work of McCain (1990). Water density at local condition is determined by:

$$\rho_w = \frac{\rho_{w\,0}}{B_w} \tag{37}$$

4.3 Gas-oil solubility and bubble point pressure

If the local pressure is above the bubble point pressure, the gas-oil solubility is equal to the GOR, otherwise the gas-oil solubility is calculate according to the correlation of Standing (1981), based on the charts of Standing (1947).

The bubble point pressure is determined based on the correlation of Velarde et al. (1999).

4.4 Oil formation volume factor and oil density

Based on the definition of oil formation volume factor:

$$B_o = \frac{\upsilon_o}{\upsilon_{o\,0}} \tag{38}$$

where υ_o and $\upsilon_{o\,0}$ is, respectively, the oil volume of a particle at local conditions and at standard conditions, the following material balance relation results:

$$B_o = \frac{\rho_{o\,0} + \dfrac{P_0\,M_a}{\Lambda\,T_0}\,R_s\,\gamma_{dg}}{\rho_o} \tag{39}$$

where $\Lambda = 8,314\, m^2\, s^{-2}\, K^{-1}$ is a universal constant.

Assuming that the black oil approximation is valid and substituting Eq. (26) in Eq. (39), we obtain:

$$B_o \cong \frac{\rho_{o0} + \rho_{g0}\, R_s}{\rho_o} \tag{40}$$

The oil density is calculated based on the correlation of Velarde et al. (1999).

4.5 Gas, oil and water viscosity

The gas viscosity is calculated using the correlation of Lee et al. (1966).

The dead oil viscosity at standard pressure is calculated using the correlation of Ng and Egboah (1994), which was based on the charts of Beal (1946). The dead oil viscosity is necessary to calculate the saturated and subsaturated oil viscosity. The former is calculated using the correlation of Beggs and Robinson (1975), which was based on the charts of Chew and Connaly Jr (1959); and the latter is calculated using the correlation of Vasquez and Beggs (1980), based on the work of Beal (1946).

The water viscosity is calculated using the results of Collins (1987). The first step is the determination of the water viscosity at standard pressure, then it is possible to evaluate the water viscosity at local conditions.

5 STATIONARY STATE

The stationary state is important since it is used as the initial condition for the transient simulations. The stationary state can be obtained by setting to zero the time derivatives in the dynamic equations. Applying this procedure to Eqs. (6), (7) and (8), we obtain respectively:

$$j_g = \frac{Q_{o0}\ (GOR - R_s)\ B_g}{A} \tag{41}$$

$$j_o = \frac{Q_{o0}\, B_o}{A} \tag{42}$$

$$j_w = \frac{Q_{o0}\, WOR\, B_w}{A} \tag{43}$$

where Q_{o0} is the oil flow rate at standard conditions, GOR is the gas-oil ratio, R_s is the solution gas-oil ratio, B is the formation factor for the fluids, A is the flow passage area of the riser tube and WOR is the water-oil ratio.

The pressure at the top of the riser is calculated through the Perkin's model:

$$P_{top} = P(w, D, D_c, T, P_{sep}, \gamma_g, API, GOR, WOR) \tag{44}$$

where w is the mass flow rate, D_c is the choke diameter, T is the fluid temperature, P_{sep} is the separator pressure and API is the API gravity.

Based on Eq. (9) and using forward difference to evaluate the spatial derivative, it is possible to calculate the pressure along the riser:

$$P_i = P_{i+1} + (s_{i+1} - s_i) \left[\frac{4\ (\tau_w)_{i+1}}{D} + g\ (sin\,\theta)_{i+1} \right] \tag{45}$$

where i represents a specific node in the static grid.

The convergence of the variable values is obtained using an iterative procedure based on the predictor-corrector method.

6 TRANSIENT STATE

To evaluate the transient state, the initial conditions are taken from the stationary state results. A moving grid method was adopted, in which node i ($1 \leq i \leq N-1$) moves with the gas characteristic velocity. Last node N moves with the liquid velocity if the liquid level falls bellow the top of the riser, or remain fixed at the top otherwise. The time step is calculated as the time step such that the node $N-1$ intersects the node N. As the gas velocity is positive, a node disappears at the liquid level or top of the riser and a node is created at the bottom of the riser, keeping constant the number of nodes. The transient calculations can be summarized as follows:

1. The predictor values of the variables j, P, α, α_o, α_w, u_g and u_l are assumed as the corresponding values obtained at time t_1.
2. The time step Δt is calculated based on the predictor values.
3. The pressure at the top of the riser is estimated based on the Perkin's model.
4. The fluid properties are calculated at the nodal positions.
5. The pressure along the riser at time $t_2 = t_1 + \Delta t$ is calculated using a implicit scheme, based on Eq. (45).
6. The gas volume fraction α at time t_2 is calculated by discretizing Eq. (30) and integrating it along the gas characteristic direction using a implicit forward scheme.
7. The oil volume fraction α_o at time t_2 is calculated by discretizing Eq. (31) and integrating it along the liquid characteristic direction using a implicit forward scheme. The values of the variables at the liquid characteristic direction is calculated by means of interpolations from the values of the variables at the gas characteristic direction.
8. The gas velocity u_g at time t_2 is determined using Eq. (22); j and u_l are also determined.
9. By knowing the corrector values, new predictor values for the variables are determined using an under-relaxation factor.
10. Steps 2 to 9 are repeated until convergence is achieved.

7 RESULTS

A computational program for transient simulations was developed and a convergence study was made, varying the number of nodes. It was observed that acceptably converged results are obtained with 101 nodes.

Two different inlet flow boundary conditions were tested, one in which the fluids superficial velocities were kept constant and other in which the liquid superficial velocity was kept constant and the gas superficial velocity was modified as a function of time. The last case tries to simulate the occurrence of flow instabilities, as in severe slugging, in which the gas flow rate increases sharply during the blowout stage.

Variable	Case 1	Case 2
API	19	19
γ_g	0.6602	0.6602
$Q_{g\,0}$	$0.1\,Sm^3/s$	$time - varying$
GOR	145	145
WOR	0.3	0.3
T	$323K$	$323K$
D	4”	4”
X	$845\,m$	$845\,m$
Z	$1300\,m$	$1300\,m$
ϵ	$4,6\,.\,10^{-5}\,m$	$4,6\,.\,10^{-5}\,m$
d	$40\,\frac{1}{64}$”	$70\,\frac{1}{64}$”
Y	0	0
N	101	101

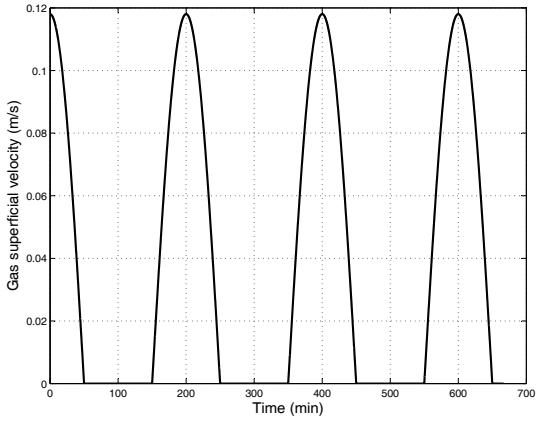

Table 1: Input data for simulations and gas superficial velocity at riser inlet for Case 2.

Table 1 presents the input data used to simulate the flow in the riser. Case 1 refers to the case in which the inlet boundary condition was kept constant during the entire simulation and Case 2 refers to the case in which the gas superficial velocity is given by the following expression:

$$j_g(t) = \begin{cases} j_{g\ stat}\,\cos\left(\frac{2\pi}{T}\,t\right), & \text{if } \ 0 \leq \frac{t}{T} \leq \frac{1}{4} \text{ or } \left(\frac{3}{4}+n\right) \leq \frac{t}{T} \leq \left(\frac{5}{4}+n\right), n \in \mathbb{N} \\ 0, & \text{if } \ \left(-\frac{3}{4}+n\right) < \frac{t}{T} < \left(-\frac{1}{4}+n\right) \end{cases} \tag{46}$$

where $j_{g\ stat}$ is the gas superficial velocity calculated at the stationary state and T is the period, chosen as $T = 200$ minutes.

Figure 2 presents the results obtained by simulating the Case 1 input data. The numerical solution oscillates during the first 500 minutes; this occurs because the computational program switches from the stationary model to the transient model after the stationary solution is calculated.

Observe that the numerical solution does not go away from the initial condition with time, therefore the stationary solution is stable and is the system steady state. If the numerical solution goes away with time, the stationary state is unstable, there is no steady state and a cyclic solution develops with time.

Observe also that after the solution stabilizes, there are some variables that are slightly different if compared with the values at time zero, however the differences are smaller than 2%; these small differences are associated to the numerical procedure used for the transient calculations.

Figure 3 presents the pressure, fluids void fraction and velocity along the riser at time 700 min, after the oscillations cease; these results can be regarded as the steady state values calculated with the transient code.

Figure 4 presents results obtained by simulating the Case 2 input data. Figure 4(a) shows that the maximum pressure at the bottom of the riser is reached a few minutes after the gas superficial velocity at the riser inlet is null. It happens mainly due to the fact that the weight of the hydrostatic column becomes heavier as the volume of gas that leaves the riser is bigger than the volume of gas that enters at the bottom plus the volume of gas that is released by vaporization; thus, the average void fraction along the riser tends to decrease. On the other hand, Fig. 4(b) shows that the maximum pressure at the top of the riser is reached a few minutes after the gas superficial velocity at the riser inlet reaches its maximum, what can be explained

due to the fact that the higher the mass flow through the choke valve, the bigger the pressure drop, leading to a pressure rise at the upstream region of the valve.

Figure 4(c) shows that although the gas superficial velocity is null at the bottom of the riser, a gas velocity can still be calculated by using the drift flux model, resulting:

$$u_g = C_d\, j + U_d \tag{47}$$

This limit velocity obtained when the gas flow rate tends to zero is used to displace the nodes; however there is no gas flux at the riser inlet, what is observed at Fig. 4(e), that shows a null gas void fraction when the gas superficial velocity is null.

Observe also that the gas velocity is greater at the top of the riser and that the gas void fraction at this position never reaches zero. This happens because of the gas vaporization as the pressure drops along the riser.

8 CONCLUSIONS AND PERSPECTIVES

The gas, oil and water flow in a catenary-shaped riser was modeled. The method of characteristics was used to calculate the compatibility conditions from a hyperbolic system of conservation equations and the obtained characteristics are real, so that the formulation proves to be well posed.

The stationary state is calculated by setting to zero the time derivatives in the dynamic equations; this result is used as initial condition to the dynamic model. If the inlet boundary condition is constant and the variables stabilizes with time, then the steady state is reached. Otherwise the stationary state is unstable, the steady state does not exist and a cyclic solution is obtained. A time-varying inlet boundary condition is simulated, showing the time response of the system to the dynamic inlet condition.

The analyzed model refers only to the riser; in order to describe a complete petroleum production system a pipeline model is being studied. The riser and pipeline models are coupled by continuity conditions. After the pipeline model is developed, it will be possible to study the severe slugging phenomenon and the stability in petroleum systems. This is a work in progress.

9 ACKNOWLEDGEMENTS

This work was supported by Petróleo Brasileiro S. A. (Petrobras). The authors wish to thank *Fundação de Amparo à Pesquisa do Estado de São Paulo* (FAPESP, Brazil) and *Conselho Nacional de Desenvolvimento Científico e Tecnológico* (CNPq, Brazil)

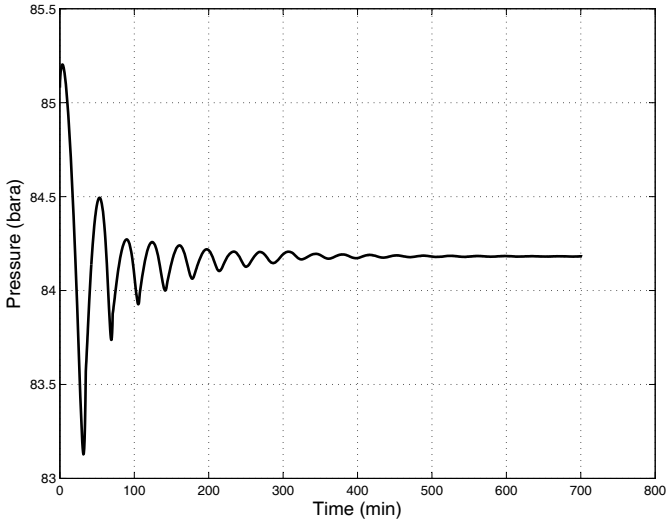

(a) Pressure at the bottom of the riser.

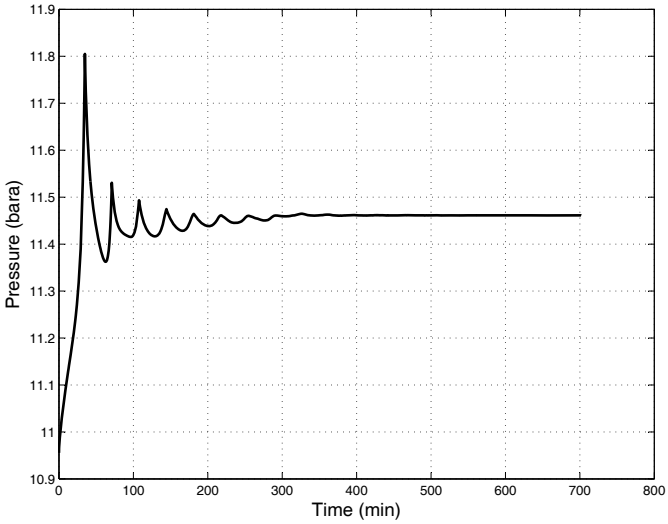

(b) Pressure at the top of the riser.

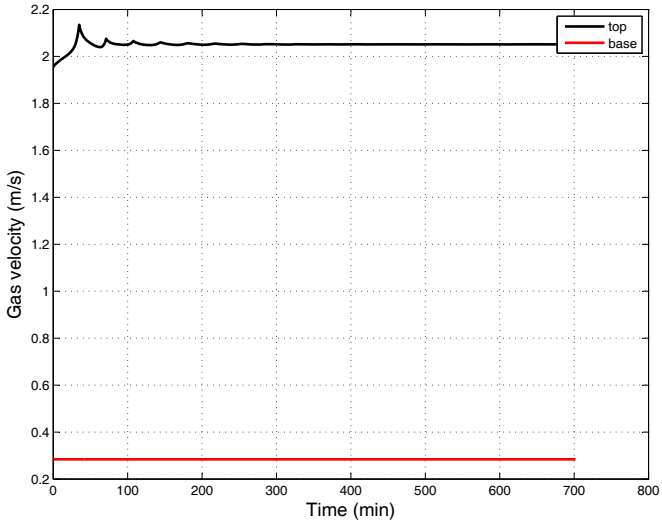

(c) Gas velocity at the bottom and top of the riser.

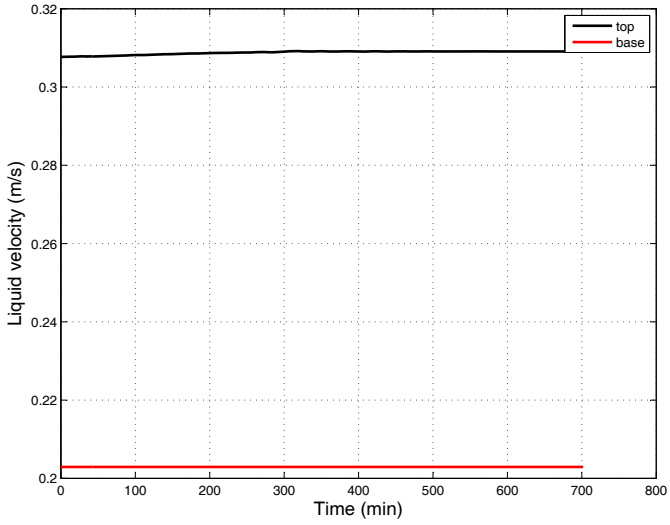

(d) Liquid velocity at the bottom and top of the riser.

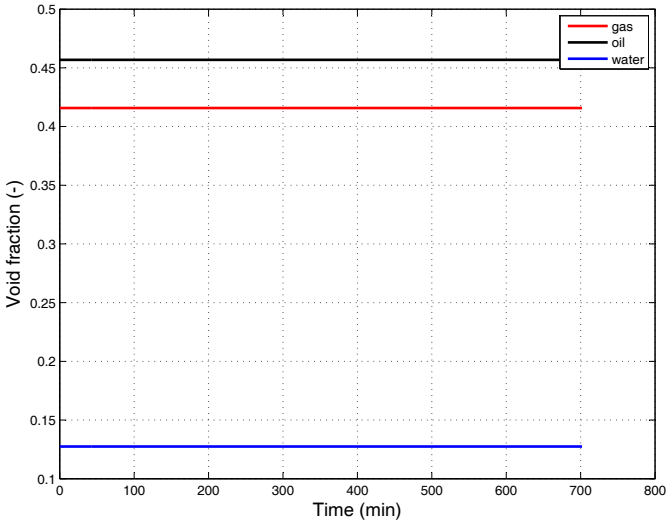

(e) Fluids void fraction at the bottom of the riser.

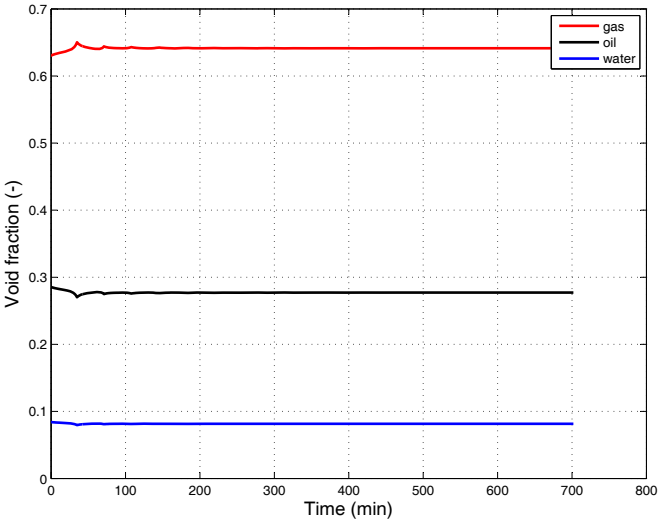

(f) Fluids void fraction at the top of the riser.

Figure 2: Simulation results of Case 1 (constant inlet boundary condition).

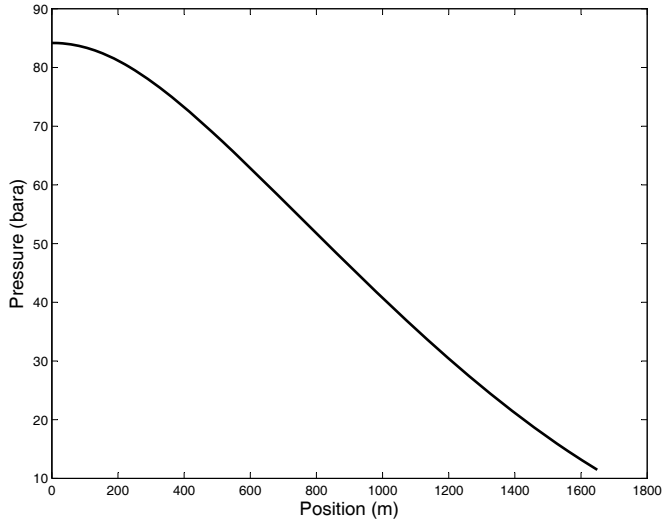

(a) Pressure along the riser.

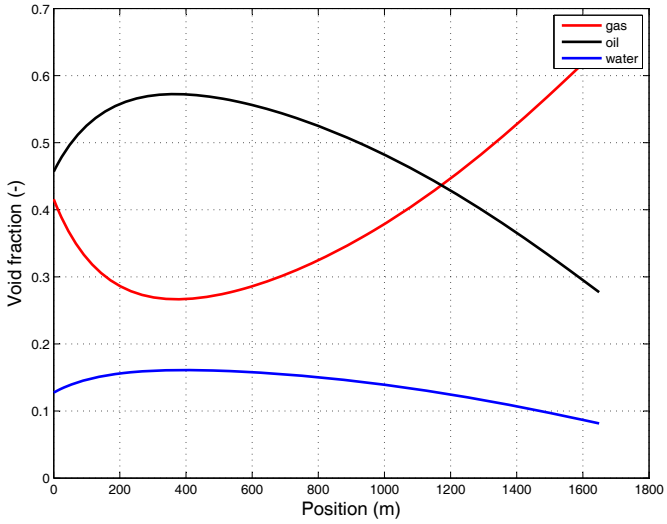

(b) Fluids void fraction along the riser.

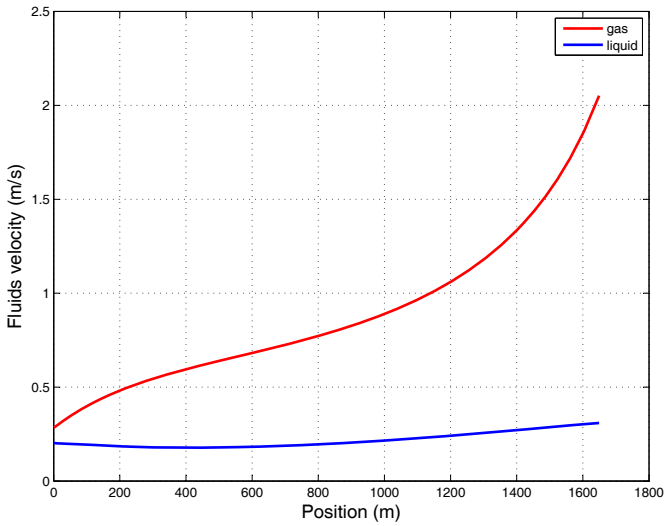

(c) Gas and liquid velocity along the riser.

Figure 3: Pressure, volume fractions and velocities along the riser at steady state.

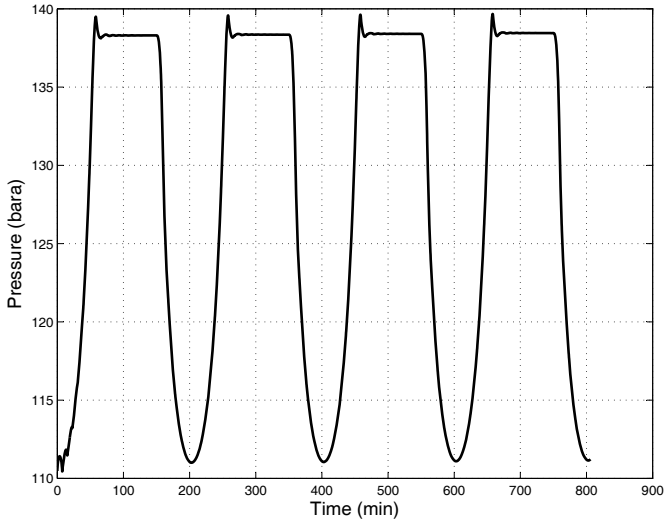

(a) Pressure at the bottom of the riser.

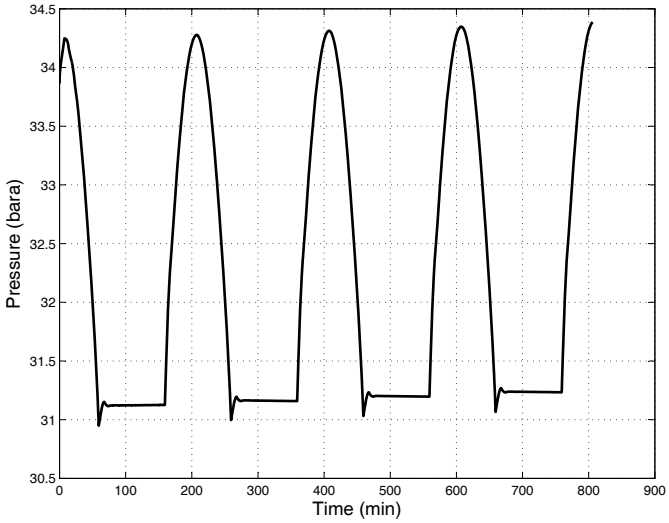

(b) Pressure at the top of the riser.

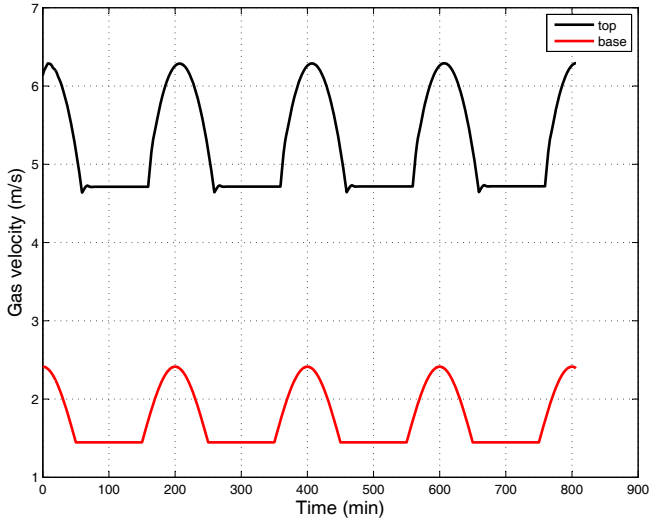

(c) Gas velocity at the bottom and top of the riser.

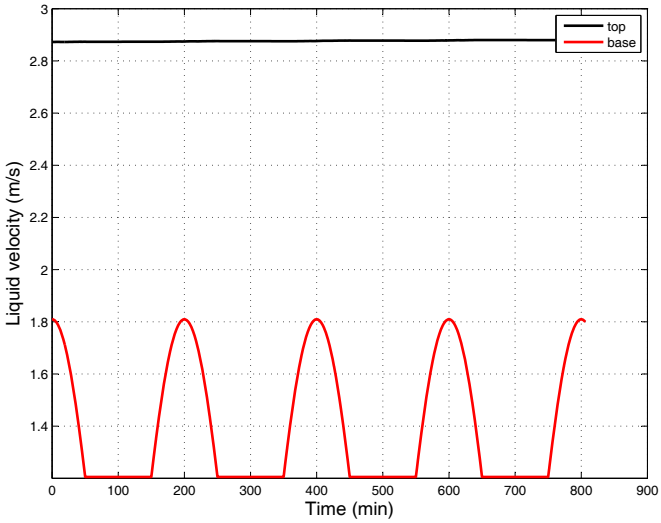

(d) Liquid velocity at the bottom and top of the riser.

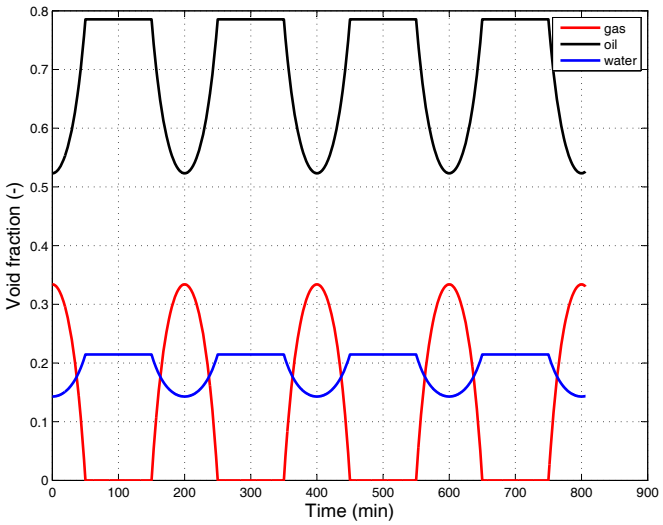

(e) Fluids void fraction at the bottom of the riser.

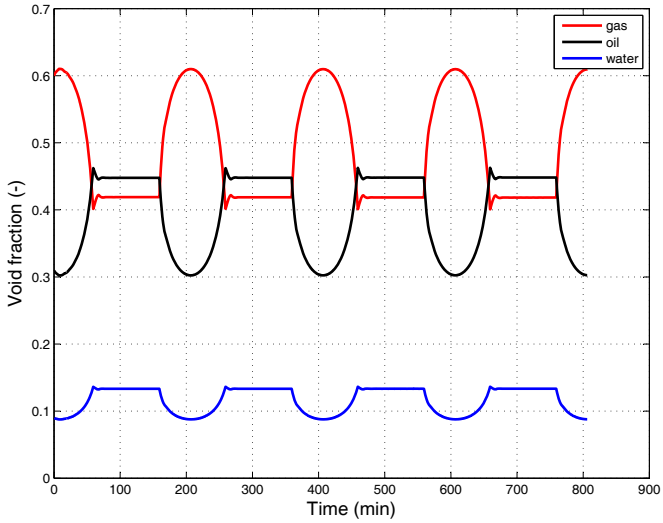

(f) Fluids void fraction at the top of the riser.

Figure 4: Simulation results of Case 2 (time-varying inlet boundary condition).

REFERENCES

Ames W.F. *Numerical methods for partial diferential equations*. Academic Press, Rio de Janeiro, 1992.

Baliño J.L., Burr K.P., and Nemoto R.H. Modeling and simulation of severe slugging in air-water pipeline-riser systems. *International journal of multiphase flow*, 36:643–660, 2010.

Beal C. The viscosity of air, water, natural gas, crude oils and its associated gases at oil field temperatures and pressures. *Trans. AIME*, 165:94–112, 1946.

Beggs H.D. and Robinson J.R. Estimating the viscosity of crude oil systems. *JPT*, pages 1140–1141, 1975.

Bendiksen K.H. An experimental investigation of the motion of long bubbles in inclined tubes. *International journal of multiphase flow*, 10(4):467–483, 1984.

Brown G.G., Katz D.L., Oberfell G.G., and Alden R.C. *Natural gasoline and the volatile hydrocarbons*. NGAA, Tulsa, 1948.

Chen N.H. An explicit equation for friction factor in pipe. *Ind. Eng. Chem. Fundam.*, 18:296–297, 1979.

Chew J. and Connaly Jr C.A. A viscosity correlation for gas-saturated crude oils. *Trans. AIME*, 216:23–25, 1959.

Chexal B., Lellouche G., Horrowitz J., and Healer J. A void fraction correlation for generalized applications. *Progress in nuclear energy*, 27(4):255–295, 1992.

Collins A.G. *Petroleum Engineering Handbook*, chapter Properties of produced waters. SPE, Dallas, 1987.

Dranchuk P.M. and Abu-Kassem J.H. Calculation of z-factors for natural gases using equations of state. *JCPT*, pages 34–36, 1975.

Drew D.A. and Passman S.L. *Theory of Multicomponent Fluids*. Springer-Verlag, New York, 1999.

Fabre J., Presson L.L., Corteville J., Odello R., and Bourgeois T. Severe slugging in pipeline/riser systems. *SPE 16846*, 5(3):299–305, 1987.

Lee A.L., Gonzalez M.H., and Eakin B.E. The viscosity of natural gases. *Trans. AIME 237*, pages 997–1000, 1966.

Masella J.M., Tran Q.H., Ferre D., and Pauchon C. Transient simulation of two-phase flows in pipes. *Int. J. Multiphase Flow*, 24:739–755, 1998.

McCain W.D. *The properties of petroleum fluids*. PennWell Books, Tulsa, 1990.

Ng J.T.H. and Egboah E.O. An improved temperature-viscosity correlation for crude oil systems. CIM, Banff, 1994.

Perkins T.K. Critical and subcritical flow of multiphase mixtures through chokes. *SPE Drilling and Completion*, pages 271–276, 1993.

Rastoin S., Schmidt Z., and Doty D.R. A review of multiphase flow through chokes. *Journal of energy resources technology*, 119:10, 1997.

Sarica C. and Shoham O. A simplified transient model for pipeline-riser systems. *Chemical Engineering Science*, 46(9):2167–2179, 1991.

Schmidt Z., Brill J., and Beggs H. Experimental study of severe slugging in a two phase flow pipeline-riser system. *SPE, Paper 8306*, 20:407–414, 1979.

Standing M.B. A pressure-volume-temperature correlation for mixtures of california oil and gases. *Drilling and Production Practice*, pages 275–287, 1947.

Standing M.B. *Volumetric and Phase Behavior of Oil Field Hydrocarbon Systems*. SPE, 9a. edição, Dallas, 1981.

Standing M.B. and Katz D.L. Density of natural gases. *Trans. AIME*, 146:140–149, 1942.

Taitel Y., Vierkand S., Shoham O., and Brill J.P. Severe slugging in a riser system: experiments and modeling. *International journal of multiphase flow*, 16(1):57–58, 1990.

Vasquez M. and Beggs H.D. Correlations for fluid physical properties prediction. *JPT*, 32:968–970, 1980.

Velarde J., Blasingame T.A., and McCain W.D. Correlation of black oil properties as pressures below bubblepoint pressure – a new approach. *Journal of Canadian Petroleum Technology*, 38(13):1–6, 1999.

Zuber N. and Findlay J. Average volumetric concentration in two-phase flow system. *Journal of Heat Transfer*, 87:453, 1965.